VOLUME 11 | ISSUE 1

HJR

Neuroradiology ORIGINAL ARTICLE

Quantitative Assessments For Phase-Sensitive Inversion Recovery Post Gadolinium Based Contrast Enhancement

Hamza Arjah[1,2], Noor Diyana Osman[1], Hussein ALMasri[3], Sawsan E. Abusharkh[4], Mustafa Hammad[5], Mohammad Nofal[6], Omarah Abdelqader[2]

[1]*Advanced Medical and Dental Institute, Universiti Sains Malaysia, Kepala Batas, Penang, Malaysia*

[2]*Radiology Department, Allmed Medical Center, Ramallah, Palestine*

[3]*Medical Imaging Department, Faculty of Health Professions, Al-Quds University, Abu dis, Jerusalem, Palestine*

[4]*Physiology and pharmacology department, Faculty of Medicine, Al-Quds University, Abu dis, Jerusalem, Palestine*

[5]*Neurology clinic, Allmed Medical Center, Ramallah, Palestine*

[6]*Al-Salihi Radiology Center, Ramallah, Palestine*

SUBMISSION: 20/01/2025 | ACCEPTANCE: 17/10/2025

ABSTRACT

Purpose: The T1-weighted Magnetization Prepared Rapid Acquisition Gradient Echo (T1 MPRAGE) sequence is widely adopted for gadolinium-based contrast enhancement (GBCE) for brain lesions, but researchers still inspect other sequences for GBCE to achieve more accurate diagnostic images. This study aimed to evaluate the effectiveness of Phase Sensitive Inversion Recovery (PSIR) in evaluating brain lesions post-GBCE.

KEY WORDS

PSIR, MRI contrast, Brain MRI, contrast-to-noise ratio (CNR), GBCE

CORRESPONDING AUTHOR, GUARANTOR

Hamza Arjah, Advanced Medical and Dental Institute, Universiti Sains Malaysia, Kepala Batas, Penang, Malaysia - Radiology Department, Allmed Medical Center, Ramallah, Palestine
Email: hamza.arejeh@gmail.com
Tel: 00972597266724

Material and Methods: Retrospective data collection from one radiology unit included 44 patients with Brain lesions. The patients underwent brain Magnetic Resonance Imaging (MRI) with GBCE using a 1.5 Tesla MRI scanner. GBCE analysis on MPRAGE and PSIR sequences involved quantitative assessments based on the contrast ratio (CR), contrast enhancement (CE), and contrast-to-noise ratio (CNR) for MPRAGE.

Results: PSIR CNR was slightly higher than T1-MPRAGE, while T1-MPRAGE was more effective in CE and CR. The average lesion CNR was 38.4 for T1-MPRAGE, and increased to 41.3 for PSIR without a significant difference p-value > 0.05. For CE, the average lesion CE in T1-MPRAGE was 0.75, and significantly decreased to 0.36 for the PSIR sequence p-value < 0.001. The CR in T1-MPRAGE exhibited an average value of 1.2, while PSIR's average value significantly decreased to 0.67, p-value < 0.001. However, the CR and CE were higher in PSIR for some lesions.

Conclusion: Although PSIR post-GBCE imaging can enhance the visualisation of certain brain lesions, in some cases, it cannot replace T1 MPRAGE for routine clinical use. However, PSIR post-GBCE can be combined with T1-MPRAGE to improve lesion evaluation.

Introduction

MRI is widely recognised for its superior soft tissue contrast and non-invasive capabilities, making it a critical diagnostic tool for brain lesion detection. PSIR is an MRI sequence that has drawn attention for its potential to enhance lesion visibility. PSIR offers improved CNR and reduces artefacts, which can help in the identification of subtle pathological changes in brain tissue [1].

PSIR imaging benefits from its phase-sensitive nature, which allows for precise tissue differentiation and improved lesion conspicuity compared to MPRAGE. The ability of PSIR to detect low signal intensity (SI) lesions or differentiate complex structures could provide a diagnostic advantage in challenging cases, such as multiple sclerosis (MS), gliomas, and metastases [2] [3] [4] [5]. The GBCE is essential for some pathologies [6]. And it should be administered according to the clinical needs [7]. However, different works employed different sequences post-GBCE, such as susceptibility-weighted imaging (SWI) [8], Fluid-Attenuated Inversion Recovery (FLAIR) [9] and PSIR [10]. Each work achieved different benefits and limitations, so selecting a new sequence post-GBCE can sometimes add benefits.

Ping Hou et al. mentioned in their work that the PSIR sequence can detect GBCE enhancement in Brain lesions [10]. No work in our literature has evaluated brain lesions for PSIR post-GBCE compared to standard T1 post-GBCE for different Brain lesions. This study addresses this challenge by comparing the diagnostic performance of PSIR post-GBCE imaging with T1 MPRAGE sequences for brain lesion evaluation and characterisation. This work employs quantitative assessment for lesions, including CE, CR, and CNR.

Methods

Scanner, Patients and Sequences

MRI scans were performed using a Siemens MAGNETOM ESSENZA 1.5 Tesla system equipped with PSIR and MPRAGE sequences. A head-and-neck 16-channel coil was used for all scans. Retrospective data collection achieved ethical approval from the institutional research and ethics review committee (413/REC/2024). Data collection included 44 patients diagnosed with various brain lesions; among these patients, 27 underwent PSIR pre-GBCE and post-GBCE imaging, while 17 received only PSIR post-GBCE. All 44 patients were scanned using T1 MPRAGE pre-GBCE and post-GBCE sequences.

Quantitative analysis

Region-of-interest (ROI) analyses were employed for both PSIR and T1-MPRAGE; lesion size and region were accounted for during analysis, with ROI placement specific to each lesion and other ROI in surrounding normal tissue. Mean signal intensity (SI) and the standard deviation (SD) values were recorded for post-GBCE and pre-GBCE sequences. The following metrics were used for quantitative analysis:

Contrast Ratio (CR)

CR was calculated according to Equation 1, and the calculation was performed on PSIR and MPRAGE post-GBCE images [11]:

$$Contrast\ Ratio\ (CR) = \frac{S_{normal}}{S_{lesion}}$$

Equation 1

Where S_{lesion} is the mean signal intensity within the lesion, S_{normal} is the mean signal intensity (SI) in the surrounding normal tissue [12].

Contrast Enhancement (CE)

CE was defined by Equation 2; the CE measurements require pre-GBCE and post-GBCE to be achieved [13].

$$Contrast\ Enhancement\ (CE) = \frac{SI_{post} - SI_{pre}}{SI_{pre}}$$

Equation 2

Where S_{Ipost} is the SI of lesion post-GBCE, and SI_{pre} is the SI of lesion pre-GBCE brain [13]. This calculation was performed for 27 patients only on PSIR due to the absence of PSIR pre-GBCE.

Contrast-to-Noise Ratio (CNR)

CNR measure two tissues or object's differentiation and the effect of noise on the differentiation; CNR was calculated according to Equation 3 on post-GBCE sequences [11].

$$CNR = \frac{SI_{lesion} - SI_{normal}}{SD_{background}}$$

Equation 3

Where $SD_{background}$ is the standard deviation (SD) of the SI in a region outside the brain (typically in air) [14], and SI_{lesion} and SI_{normal} are the SI values of the lesion and surrounding normal tissue, respectively. The work published by Qing Fu et al. employed the white matter (WM) as normal tissue (SInormal), and in their second measurement, they employed the grey matter (GM) as normal tissue [5]. In this work, we used WM as SInormal only because WM appears bright on T1, and contrast media also appears bright. We aim to measure CNR between two bright tissues.

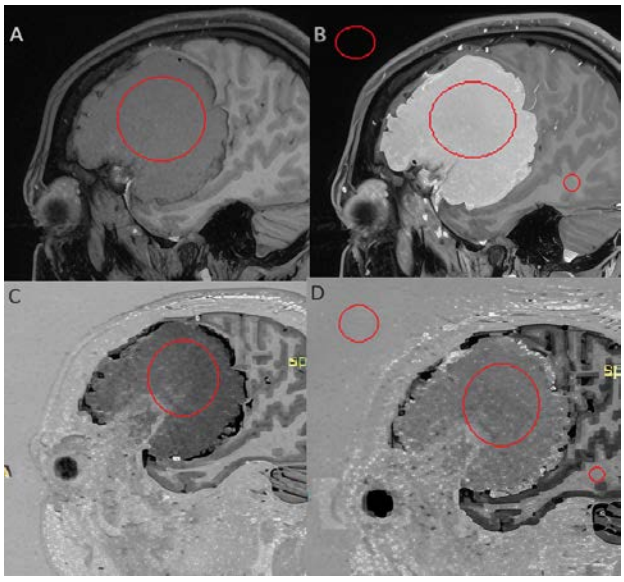

Figure 1: *Regions of interest (ROIs) in different imaging sequences: (A) T1 MPRAGE pre-GBCE illustrating the lesion; (B) T1 MPRAGE post-GBCE displaying enhancement of the lesion; (C) PSIR pre-GBCE image; (D) PSIR post-GBCE image demonstrating slight lesion enhancement and prominent wall enhancement.*

Quantitative measurements were carried out using RADIANT DICOM viewer software, with ROIs placed over lesion, background, and normal WM as depicted in Figure 1. The ROIs placed on lesions varied according to lesion size to minimise variability in SI due to different compositions and to avoid including normal tissue. At the same time, ROIs placed on normal tissue were placed on nearby WM tissue. The background noise or SD was measured using ROIs placed between bone and image border, with appropriate size to eliminate SD fluctuations within the measured areas.

The measured SI and SD of different lesions on both sequences were arranged in Microsoft Excel, and the SI and SD were employed to measure CR, CE, and CNR according to the suggested equations. A statistical t-test was performed to compare CR, CE, and CNR of both sequences, with a p-value of 0.001 considered a significant difference.

Results

Contrast ratio (CR)

The CR for the MPRAGE sequence was significantly higher compared to the PSIR sequence ($p < 0.001$). The CR values for PSIR ranged from 1.2 to 0.18, with an average of 0.67, while the CR values for MPRAGE ranged from 0.88 to 3.4, with an average of 1.7.

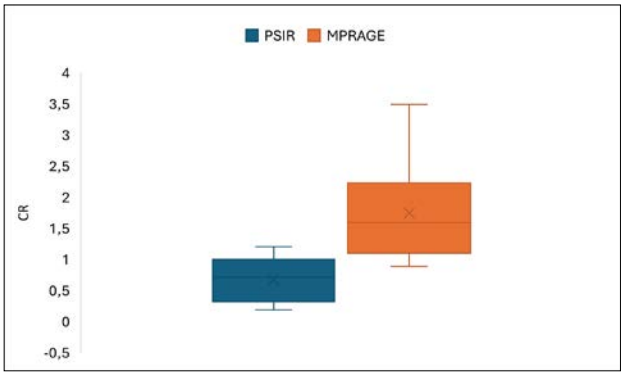

Figure 2: *The contrast ratio (CR) for the lesion, comparing values obtained from the MPRAGE and PSIR sequences.*

Contrast enhancement (CE)

MPRAGE also demonstrated significantly higher contrast enhancement (CE) compared to PSIR ($p < 0.001$). MPRAGE CE values ranged from 0.0 to 2.4, with an average of 0.75, while PSIR CE values ranged from 0.00 to 0.81, with an average of 0.36.

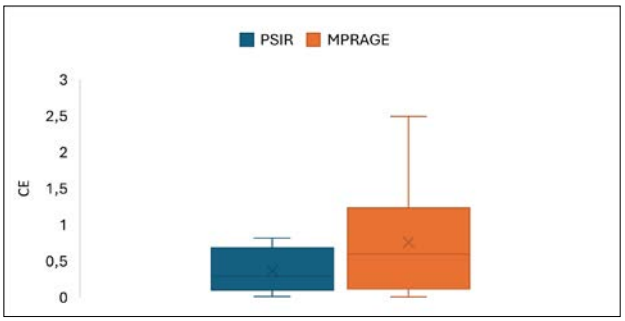

Figure 3: *Contrast enhancement (CE) for the lesion, as observed in both the MPRAGE and PSIR sequences.*

Contrast to noise ratio (CNR)

There was no significant difference between MPRAGE and PSIR in terms of the CNR ($p > 0.05$). MPRAGE CNR values ranged from 1.5 to 264.6, with an average of 38.3, while PSIR CNR values ranged from 3.1 to 170.8, with an average of 41.5.

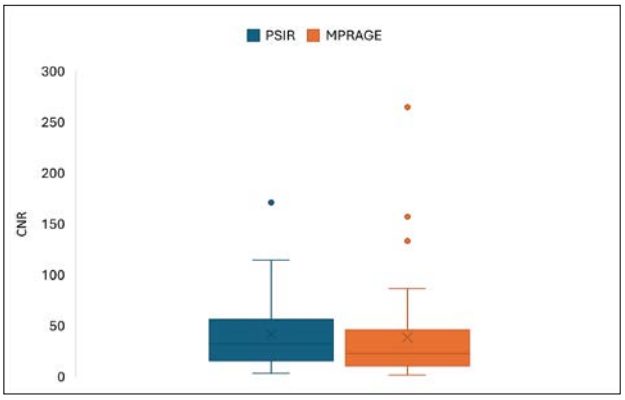

Figure 4: *Figure 4 Contrast to noise ratio (CNR) for the lesion, the results from the MPRAGE and PSIR sequences post-GBCE.*

Discussion

The findings of this study demonstrate that MPRAGE post-GBCE imaging generally provides better CE and lesion visibility than PSIR for most brain lesions. The superiority of MPRAGE can be attributed to its dark background and dark bone signals, as shown in Figures 5, 6, and 7. The dark background and bone allow for enhanced lesions by GBCE to stand out more distinctly [15]. This aligns with existing literature, where T1-weighted post-GBCE sequences like MPRAGE are routinely used for their ability to highlight GBCE that accumulate in lesions [16] [17].

However, the assessments reveal that PSIR has worsened specific scenarios. For example, in vestibular schwannomas, the bright bone hides the enhanced lesion that extends from the auditory nerve. In contrast, in some cases of MS lesions, PSIR provided better lesion border delineation and higher CR. In some cases, the differentiation between active and inactive MS lesions was more pronounced in PSIR images, as shown in Figure 5. However, the differentiation between active and inactive MS is a clinical concern [7], [18], and researchers are still developing new techniques to differentiate between active and inactive MS [2], [19], [20]. The obtained results in this work add benefits in distinguishing between active and inactive MS.

Contrast Ratio (CR)

Overall, the CR was higher for MPRAGE, indicating superior lesion GBCE. However, in certain MS cases,

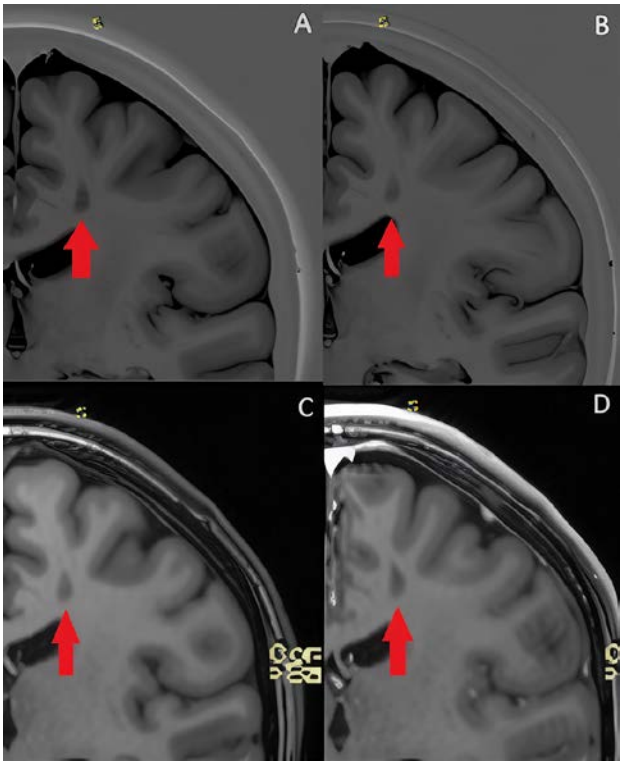

Figure 5: *Displays an MS case with imaging across four sequences: (A) PSIR pre-GBCE, (B) PSIR post-GBCE, (C) MPRAGE pre-GBCE, and (D) MPRAGE post-GBCE.*

presented in Figure 5, the visualisation of active MS enhanced by GBCE is more evident in PSIR than in MPRAGE.

This finding suggests that it may be more effective in visualising active MS lesions in some cases. However, PSIR's efficiency in detecting MS lesions without GBCE is conducted by different works [3], [21], [22]. Our results showed the ability of PSIR to differentiate between active and inactive MS lesions in PSIR post-GBCE. Previous research has also noted the strong correlation between contrast enhancement and clinical outcomes [15], and the Improvement of diagnostic precision is essential in MS [23].

Contrast Enhancement (CE)

The enhanced conspicuity of GBCE in MPRAGE sequences allows for more precise differentiation of lesion components, which is particularly important in assessing lesion vascularity [24] [25]. Ping Hou et al. concluded that the PSIR sequence is less sensitive to small T1 values such as GBCE [10], their work results support our findings, and the detection of contrast enhancement using PSIR is less than T1 MPRAGE. MPRAGE outperformed PSIR for most lesion types, except for some lesions. As shown in Figure 6, the lesion in the PSIR sequence displays better contrast enhancement than the MPRAGE sequence. Figure 6 demonstrates that the lesion is brighter with a higher signal.

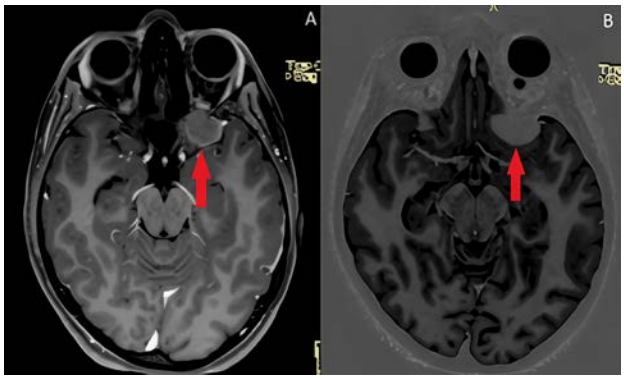

Figure 6: *Comparison of an enhanced lesion imaged using two sequences: (A) MPRAGE post-GBCE, and (B) PSIR post-GBCE.*

Contrast-to-Noise Ratio (CNR)

The WM to GM CNR was higher in PSIR compared to other T1 sequences without GBCE [10]. In this work, lesion CNR in PSIR post-GBCE was higher due to a lower noise index (SD). In contrast, the SI of enhanced lesions in T1-MPRAGE was higher. However, the final results of Equation 3 indicate a higher CNR for PSIR compared to T1 MPRAGE. The PSIR sequence suppresses the oedematous tissue beside the lesion. The lesion visibility and CNR are enhanced due to more signal differences between the suppressed dark area around the enhanced tissue by GBCE, as shown in Figure 7.

PSIR suppresses oedematous tissues surrounding lesions while enhancing lesion borders, making it particularly valuable in some instances, such as glioblastomas (GBM) and cystic schwannomas. However, the visualisation of brain oedema is critical [26] because oedematous tissue can be treated and become healthy after neurosurgery [27].

The suppressed oedematous tissue and enhanced lesion spots-GBCE are expected to help the neurosurgeon in the surgery plan for brain lesions. In addition, PSIR enhances differentiation between WM and GM, which is essential in identifying brain anatomy [3].

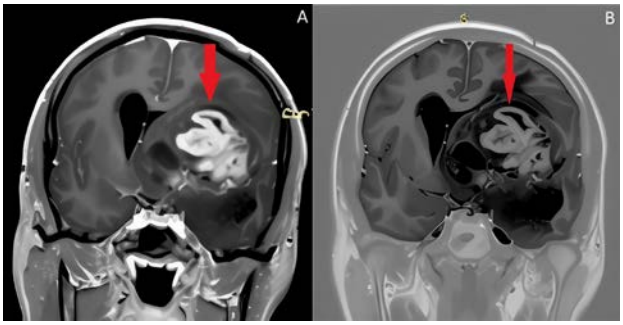

Figure 7: *Comparative imaging of glioblastomas (GBM) using two post-GBCE sequences: (A) MPRAGE post-GBCE, which provides a conventional representation of the lesion, and (B) PSIR post-GBCE, which offers an alternative GBCE-enhanced view for better delineation of tumour margins.*

The diagnostic limitations of PSIR were evident when evaluating tumours near bright structures, such as bone. The bright signal from the bone in PSIR images often obscured the lesion, making it challenging to differentiate between the lesion, the bone, and the background. The lesion should be intra-axial to avoid these limitations. MPRAGE, with its dark background, provided superior visualisation of particular lesions, such as vestibular schwannomas extending into the internal auditory canal, which was more easily visualised on MPRAGE compared to PSIR, where the dark bone signal did not interfere with lesion visibility.

This study's primary limitation is the relatively small sample size of 44 patients, which may not fully represent all brain lesion types.

Additionally, not all patients underwent PSIR pre-GBCE, so CE in 17 cases was not assessed. Further studies with larger patient populations and complete imaging datasets will be necessary to fully validate these findings and explore the complementary roles of MPRAGE and PSIR in clinical practice.

Also, we recommend including histopathology lap results with classification of CR, CE, and CNR according to pathology, as well as qualitative assessments by boarded radiologists to offer better background knowledge about PSIR post-GBCE.

Conclusion

While MPRAGE post-GBCE remains the superior sequence for most lesions, PSIR shows promise as a supplementary tool for specific lesion types like MS, cystic Schwannoma, and GBM, particularly in cases where lesion background is suppressed, and precise border delineation is crucial. Combining both sequences could offer clinicians a more comprehensive diagnostic approach, improving lesion detection and characterisation in various brain pathologies. **R**

Acknowledgments

All authors thank Allmed Medical Center for their collaboration in data collection.

References

1. V. Sethi et al., "Improved detection of cortical MS lesions with phase-sensitive inversion recovery MRI," J. Neurol. Neurosurg. Psychiatry, vol. 83, no. 9, pp. 877-882, Sep. 2012, doi: 10.1136/jnnp-2012-303023.
2. R. Nistri, A. Ianniello, V. Pozzilli, C. Giannì, and C. Pozzilli, "Advanced MRI Techniques: Diagnosis and Follow-Up of Multiple Sclerosis," Diagnostics, vol. 14, no. 11, p. 1120, May 2024, doi: 10.3390/diagnostics14111120.
3. H. Hashemi et al., "Comparison of Phase-Sensitive Inversion Recovery and Conventional Magnetic Resonance Imaging for Detection of Cortical Plaques in MS Patients," Iran. J. Radiol., vol. 18, no. 3, p. e112129, Sep. 2021, doi: 10.5812/iranjradiol.112129.
4. A. Traboulsee and D. K. B. Li, "Routine MR Imaging Protocol and Standardization in Central Nervous System Demyelinating Diseases," Neuroimaging Clin. N. Am., vol. 34, no. 3, pp. 317-334, Aug. 2024, doi: 10.1016/j.nic.2024.03.002.
5. Q. Fu et al., "Comparison of contrast-enhanced T1-weighted imaging using DANTE-SPACE, PETRA, and MPRAGE: a clinical evaluation of brain tumors at 3 Tesla.," Quant. Imaging Med. Surg., vol. 12, no. 1, pp. 592-607, Jan. 2022, doi: 10.21037/qims-21-107.
6. M. Bendszus, A. Laghi, J. Munuera, L. N. Tanenbaum, B. Taouli, and H. C. Thoeny, "Gadolinium-Based Contrast Media: Meeting Radiological, Clinical, and Environmental Needs," J. Magn. Reson. Imaging, vol. 60, no. 5, pp. 1774-1785, Jan. 2024, doi: 10.1002/jmri.29181.
7. À. Rovira et al., "Use of gadolinium-based contrast agents in multiple sclerosis: a review by the ESMRMB-GREC and ESNR Multiple Sclerosis Working Group," Eur. Radiol., vol. 34, no. 3, pp. 1726-1735, Sep. 2023, doi: 10.1007/s00330-023-10151-y.
8. M. Mugnai, E. Auriemma, B. Contiero, D. Franchini, E. Zini, and F. Tirrito, "Effect of gadolinium contrast medium administration on susceptibility-weighted imaging of the canine brain," Vet. Radiol. Ultrasound, vol. 65, no. 5, pp. 539-546, Sep. 2024, doi: 10.1111/vru.13395.
9. C. Heyn et al., "Gadolinium Enhanced T2 FLAIR is an Imaging Biomarker of Radiation Necrosis and Tumor Progression in Patients with Brain Metastases.," AJNR. Am. J. Neuroradiol., p. ajnr.A8431, Aug. 2024, doi: 10.3174/ajnr.A8431.
10. P. Hou, K. M. Hasan, C. W. Sitton, J. S. Wolinsky, and P. A. Narayana, "Phase-sensitive T1 inversion recovery imaging: a time-efficient interleaved technique for improved tissue contrast in neuroimaging.," AJNR. Am. J. Neuroradiol., vol. 26, no. 6, pp. 1432-8, 2005, [Online]. Available: http://www.ncbi.nlm.nih.gov/pubmed/15956512
11. J. Biswas et al., "Brain Tumor Enhancement in Magnetic Resonance Imaging," Invest. Radiol., vol. 40, no. 12, pp. 792-797, Dec. 2005, doi: 10.1097/01.rli.0000187609.78338.dc.
12. D. W. McRobbie, E. A. Moore, M. J. Graves, and M. R. Prince, MRI from Picture to Proton, 3rd ed. Cambridge University Press, 2017. doi: 10.1017/9781107706958.
13. R. K. Downs, M. H. Bashir, C. K. Ng, and J. O. Heidenreich, "Quantitative contrast ratio comparison between T1 (TSE at 1.5T, FLAIR at 3T), magnetization prepared rapid gradient echo and subtraction imaging at 1.5T and 3T.," Quant. Imaging Med. Surg., vol. 3, no. 3, pp. 141-6, Jun. 2013, doi: 10.3978/j.issn.2223-4292.2013.05.02.

14. O. Dietrich, J. G. Raya, S. B. Reeder, M. F. Reiser, and S. O. Schoenberg, "Measurement of signal-to-noise ratios in MR images: Influence of multichannel coils, parallel imaging, and reconstruction filters," J. Magn. Reson. Imaging, vol. 26, no. 2, pp. 375-385, Aug. 2007, doi: 10.1002/jmri.20969.
15. A. Falk Delgado et al., "Diagnostic value of alternative techniques to gadolinium-based contrast agents in MR neuroimaging—a comprehensive overview," Insights Imaging, vol. 10, no. 1, p. 84, Dec. 2019, doi: 10.1186/s13244-019-0771-1.
16. T. K. Chung, C. H. Lee, J. Lee, J. W. Choi, K. A. Kim, and C. M. Park, "Usefulness of Postcontrast T2-Weighted Images in Shortening the Total Scan Time of a Gadoxectic Acid Enhanced MRI of the Liver: a Comparison between Precontrast and Postcontrast T2-Weighted Images," J. Korean Soc. Radiol., vol. 62, no. 3, p. 249, 2010, doi: 10.3348/jksr.2010.62.3.249.
17. K. Karimian-Jazi et al., "Diagnostic value of gadolinium contrast administration for spinal cord magnetic resonance imaging in multiple sclerosis patients and correlative markers of lesion enhancement," Mult. Scler. J. - Exp. Transl. Clin., vol. 7, no. 4, p. 205521732110479, Oct. 2021, doi: 10.1177/20552173211047978.
18. R. Afkandeh, I. Abedi, and M. Zamanian, "Detection of multiple sclerosis lesions by susceptibility-weighted imaging-A systematic review and meta-analyses.," Clin. Radiol., vol. 0, no. 0, Sep. 2024, doi: 10.1016/j.crad.2024.09.009.
19. F. Bagnato et al., "Imaging chronic active lesions in multiple sclerosis: a consensus statement," Brain, vol. 147, no. 9, pp. 2913-2933, Sep. 2024, doi: 10.1093/brain/awae013.
20. A. Amini et al., "Deep learning for discrimination of active and inactive lesions in multiple sclerosis using non-contrast FLAIR MRI: A multicenter study," Mult. Scler. Relat. Disord., vol. 87, p. 105642, Jul. 2024, doi: 10.1016/j.msard.2024.105642.
21. A. Favaretto, D. Poggiali, A. Lazzarotto, G. Rolma, F. Causin, and P. Gallo, "The Parallel Analysis of Phase Sensitive Inversion Recovery (PSIR) and Double Inversion Recovery (DIR) Images Significantly Improves the Detection of Cortical Lesions in Multiple Sclerosis (MS) since Clinical Onset," PLoS One, vol. 10, no. 5, p. e0127805, May 2015, doi: 10.1371/journal.pone.0127805.
22. F. Nelson, A. H. Poonawalla, P. Hou, F. Huang, J. S. Wolinsky, and P. A. Narayana, "Improved Identification of Intracortical Lesions in Multiple Sclerosis with Phase-Sensitive Inversion Recovery in Combination with Fast Double Inversion Recovery MR Imaging," Am. J. Neuroradiol., vol. 28, no. 9, pp. 1645-1649, Oct. 2007, doi: 10.3174/ajnr.A0645.
23. P. Maggi, M. Absinta, A. J. Gill, E. M. Schorr, S. P. Gadani, and P. A. Calabresi, "Emerging MRI biomarkers for the diagnosis of multiple sclerosis," Mult. Scler. J., vol. 53, no. 8, p. e2250228, Nov. 2024, doi: 10.1177/13524585241293579.
24. Y. Kato et al., "Usefulness of Contrast-Enhanced T1-Weighted Sampling Perfection with Application-Optimized Contrasts by Using Different Flip Angle Evolutions in Detection of Small Brain Metastasis at 3T MR Imaging: Comparison with Magnetization-Prepared Rapid Acquisition," Am. J. Neuroradiol., vol. 30, no. 5, pp. 923-929, May 2009, doi: 10.3174/ajnr.A1506.
25. H. Cebeci, M. Gencturk, Y. Koksel, and D. Nascene, "Contrast enhancement in cerebral adrenoleukodystrophy: a comparison of T1 TSE and MPRAGE sequences," Jpn. J. Radiol., vol. 40, no. 12, pp. 1241-1245, Dec. 2022, doi: 10.1007/s11604-022-01309-7.
26. K. Pierzchala, A. Hadjihambi, J. Mosso, R. Jalan, C. F. Rose, and C. Cudalbu, "Lessons on brain edema in HE: from cellular to animal models and clinical studies," Metab. Brain Dis., vol. 39, no. 3, pp. 403-437, Aug. 2023, doi: 10.1007/s11011-023-01269-5.
27. S. Y. Sim and C.-Y. Choi, "Delayed cerebral edema: Possible association with an inflammatory foreign body reaction," Interdiscip. Neurosurg., vol. 25, p. 101207, Sep. 2021, doi: 10.1016/j.inat.2021.101207.

READY - MADE CITATION

Hamza Arjah, Noor Diyana Osman, Hussein ALMasri, Sawsan E. Abusharkh, Mustafa Hammad, Mohammad Nofal, Omarah Abdelqader. Quantitative Assessments For Phase-Sensitive Inversion Recovery Post Gadolinium Based Contrast Enhancement, *Hell J Radiol 2026*; 11(1): 31-37.